Molecular Therapy
Nucleic Acids
Original Article

CS-PEI/Beclin-siRNA Downregulate Multidrug Resistance Proteins and Increase Paclitaxel Therapeutic Efficacy against NSCLC

Wangta Liu,[1,9] Yu-Lun Lo,[2,3,9] Chin Hsu,[3,4] Yi-Ting Wu,[2] Zi-Xian Liao,[5] Wen-Jeng Wu,[4,6] Yi-Jou Chen,[7] Chieh Kao,[8] Chien-Chih Chiu,[1,4] and Li-Fang Wang[2,4,5]

[1]Department of Biotechnology, College of Life Sciences, Kaohsiung Medical University, Kaohsiung 807, Taiwan; [2]Department of Medicinal and Applied Chemistry, College of Life Sciences, Kaohsiung Medical University, Kaohsiung 807, Taiwan; [3]Department of Physiology, Faculty of Medicine, College of Medicine, Kaohsiung Medical University, Kaohsiung 807, Taiwan; [4]Department of Medical Research, Kaohsiung Medical University Hospital, Kaohsiung 807, Taiwan; [5]Institute of Medical Science and Technology, National Sun Yat-Sen University, Kaohsiung 804, Taiwan; [6]Department of Urology, School of Medicine, College of Medicine, Kaohsiung Medical University, Kaohsiung 807, Taiwan; [7]School of Medicine, Chang Guan University, Taoyuan City 33302, Taiwan; [8]School of Medicine for International Students, I-Shou University, Kaohsiung 82445, Taiwan

Paclitaxel (PTX) is a widely used chemotherapy drug; however, frequent use causes multidrug resistance (MDR), which limits the utility of PTX against advanced non-small-cell lung cancer (NSCLC). PTX-resistant subline (NCI-H23-TXR) was established *in vitro* by exposing NCI-H23 cells to gradually increased concentrations of PTX in culture medium. Distinct Beclin expression of autophagy level was observed between resistant NCI-H23-TXR and parental NCI-H23 cells. Beclin-small interfering RNA (siRNA) was selected to restore sensitivity of PTX against NCI-H23-TXR. Chondroitin sulfate-polyethylenimine (CS-PEI) was constructed for delivery and protection of Beclin-siRNA. To delineate the underlying molecular mechanism of Beclin knockdown, we analyzed different MDR expression proteins of two cells using western blot, and the corresponding genes were confirmed by real-time PCR. Compared with NCI-H23, NCI-H23-TXR had higher expression levels in P-glycoprotein (P-gp) and multidrug resistance protein 7 (ABCC10). Knockdown of Beclin simultaneously inhibited P-gp and ABCC10, and renewed the sensitivity of PTX against NCI-H23-TXR. Research on zebrafish embryos revealed that tumor sizes decreased in NCI-H23 tumor xenografts but remained intact in NCI-H23-TXR tumor xenografts as zebrafish were treated with 1 μg/mL PTX. In contrast, the tumor sizes decreased in NCI-H23-TXR tumor xenografts with zebrafish pre-transfected with CS-PEI/Beclin-siRNA followed by the same treatment of PTX. The role of autophagy was associated with MDR development. This study paves the way for a new avenue of PTX in MDR-related lung cancer therapy using CS-PEI as a gene delivery carrier.

INTRODUCTION

Lung cancer is generally diagnosed at a late stage because its symptoms are similar to breathing diseases. Although various lung cancer diseases respond well to chemotherapy, repeated treatment with single-drug agents results in resistance to chemotherapy or development of multidrug resistance (MDR).[1] In addition, conventional single-drug chemotherapy involves severe side effects such as vomiting, dizziness, and hair loss because of the high dosage and multi-administration required.[2]

Paclitaxel (PTX) is a tubulin-disrupting agent and a first-line chemotherapy drug in the treatment of advanced non-small-cell lung cancer (NSCLC).[3] To improve the therapeutic outcome of PTX for lung cancer chemotherapy, finding an alternative approach to solving MDR problems is essential.[4–6] One of the key factors influencing chemoresistance of cells to PTX is overexpression of P-glycoprotein (P-gp; MDR1), which works as a drug efflux pump.[1] Direct reduction of P-gp expression by inhibitors seems to be a straightforward strategy; however, such a strategy is associated with a toxic problem at the dosage required to attenuate P-gp function in clinical settings.[4,7] Moreover, there is another hurdle of PTX, because resistant mechanisms are complicated and remain largely unknown. The use of autophagy to regulate programmed cell death in MDR cells has received increasing attention.

Treating NSCLC with nanoparticle-mediated small interfering RNA (siRNA) seems attractive[2,8–10] because of its ability to selectively regulate problematic genes in a sequence-dependent manner. Combinations of chemotherapy drugs and gene drugs have been considered

Received 20 March 2019; accepted 18 June 2019;
https://doi.org/10.1016/j.omtn.2019.06.017.

[9]These authors contributed equally to this work.

Correspondence: Li-Fang Wang, Department of Medicinal and Applied Chemistry, College of Life Sciences, Kaohsiung Medical University, 100, Shih-Chuan 1st Rd, Kaohsiung City 807, Taiwan.
E-mail: lfwang@kmu.edu.tw
Correspondence: Chien-Chih Chiu, Department of Biotechnology, College of Life Sciences, Kaohsiung Medical University, 100, Shih-Chuan 1st Rd, Kaohsiung City 807, Taiwan.
E-mail: cchiu@kmu.edu.tw

as an innovative strategy to overcome MDR in treating NSCLC; however, most studies focused on the use of PTX combined with MDR-related siRNA[11] or tumor-associated siRNA to improve tumor suppression efficacy.[10,12–14] Few used autophagy-related siRNA to promote inhibition of MDR-related proteins and to renew the sensitivity of drug-resistant cells to PTX.[15]

Autophagy is the naturally regulated mechanism of cells that degrades unwanted or dysfunctional components. Autophagy responds to various types of stress, including hypoxia, starvation, and DNA damage,[16,17] which disassembles dysfunctional proteins and organelles to yield more energy for adaptation to adverse environments and avoidance of cell apoptosis.[18] In contrast, cell death is inhibited by suppressing expression of vital autophagy-associated genes.[19,20] The function of autophagy seems to be a double-edged sword that can be employed to protect or to kill tumor cells, depending on the developmental stage of a cancer disease and its tumor microenvironment.[20] Several important autophagy-associated genes including Beclin,[21] Raptor, and Rictor[22] play important roles in the control of MDR in cancer.

Impaired autophagy that makes cancer cells sensitive to therapies seems a promising strategy to enhance the efficacy in treating cancer diseases,[15,23,24] if cancer cells activate the autophagy program for self-preservation. Many researchers have used small molecular inhibitors to suppress activities of autophagy-related proteins. For example, Liang et al.[25] selected 3-methyladenine and chloroquine as autophagy inhibitors to sensitize MDR-phenotype ovarian cancer SKVCR cells to vincristine. Hung et al.[26] used synthetic beta-nitrostyrene derivative CYT-Rx20 co-treated with chloroquine or bafilomycin A1 to synergistically induce breast cancer cell death.

The NCI-H23 cell line is an NSCLC. PTX-resistant sublines (NCI-H23-TXR) were established by means of long-term PTX-exposed cultures.[27] Instead of using these small autophagy inhibitors that might cause serious cytotoxicities, we first checked distinct expression of autophagy level between NCI-H23-TXR and parental NCI-H23 cells. Among autophagy-related proteins tested, Beclin showed the greatest enhancement in NCI-H23-TXR cells. Beclin plays an important role in autophagy in mammalian cells, and it functions as a scaffold for the formation of the phosphatidylinositol 3-kinase (PI3K) complex, one of the first elements recruited during the formation of autophagosomes.[28] Hence, specific Beclin-siRNA was selected as an autophagy inhibitor to restore sensitivity of NCI-H23-TXR cells to PTX. In addition, an artificially made chondroitin sulfate-polyethylenimine (CS-PEI) was utilized to deliver and protect Beclin-siRNA. CS-PEI is a low-cytotoxicity, high-efficiency, cationic polymer-based gene delivery carrier that shows CD44 targeting.[29]

Differential MDR-expressed proteins were analyzed using western blot, and their corresponding genes were analyzed using real-time PCR between NCI-H23 and NCI-H23-TXR cells treated with Beclin-siRNA and/or PTX. To account for the restored sensitivity of NCI-H23-TXR to PTX after treatments, we examined cell viability using the 3-(4,5-dimethyl-2-thiazolyl)-2,5-diphenyltetrazolium bromide (MTT) assay, and cell apoptosis was analyzed using the Annexin V-PI (propidium iodide) dual-staining assay and micro-western array analysis. The re-sensitization of NCI-H23-TXR cells to PTX was also confirmed using a zebrafish embryo model.

RESULTS

Synthesis and Characterization of CS-PEI

CS-PEI was synthesized as previously reported.[29] The ^{1}H-NMR (proton nuclear magnetic resonance) spectrum implied successful synthesis of CS-PEI (Figure S1A), and the grafting percentage of PEI onto CS was ~78 wt% calculated according to the decrease in primary amino groups from its parental PEI.[30] CS-PEI could well encapsulate with siRNA at a nitrogen-to-phosphorus (N/P) ratio exceeding 5 because no naked siRNA was observed by agarose gel electrophoresis (Figure S1B). No obvious cytotoxicity of CS-PEI/siRNA was observed at N/P ratios within 1–9 against NCI-H23, NCI-H23-TXR, and 3T3 cells (Figure S1C). The transmission electron microscopy (TEM) images of CS-PEI/siRNA showed sizes of polyplexes all less than 100 nm as N/P ratios exceeding 5. The sizes were estimated to be 93.7 ± 23.4, 66.0 ± 21, and 74.2 ± 22 nm to CS-PEI/siRNA at N/P = 5, 7, and 9, respectively (Figure S1D). Particle size of a polyplex is a major factor that determines the extravasation rate of the particle from the bloodstream and recognition by the reticuloendothelial system. The polyplex with size less than 100 nm is beneficial for *in vivo* delivery.[31]

Because similar expression levels of Beclin, LC3, and ABCC10 proteins were obtained using western blot with polyplexes of N/P ratios ranging within 5–9 (Figure S2), the lowest amount of CS-PEI that offered sufficient protection of siRNA at the N/P ratio of 5 was selected for all subsequent tests to minimize cytotoxicity caused by PEI.

Characterization of PTX Resistance in NCI-H23-TXR Cells

An MTT assay was performed to validate PTX resistance of NCI-H23-TXR cells. As shown in Figure 1A, the half maximal inhibitory concentration (IC_{50}) value of PTX was 5.680 ng/mL against NCI-H23 cells but as high as 1,296 ng/mL against NCI-H23-TXR cells for 3 days post-incubation. The cell viabilities of parental and resistant NCI-H23 cells at various post-incubation days were also included in Figure S3. Following 1 day post-incubation, there was no big difference in IC_{50} value between NCI-H23 (2,128 ng/mL PTX) and NCI-H23-TXR (3,001 ng/mL PTX); nevertheless, the IC_{50} value of NCI-H23-TXR was more than 200-fold higher than that of NCI-H23 after 3 days post-incubation, indicating greater resistance in NCI-H23-TXR to PTX. Thus, 3 days post-incubation was adopted for subsequent testing unless otherwise stated.

The western blot assay was utilized to identify differentially expressed autophagy proteins in cell lines. As seen in Figure 1B, the greatest difference in Beclin and microtubule-associated protein 1 light chain 3 (LC3) expression was observed between NCI-H23 and NCI-H23-TXR cells. LC3 is involved in autophagosome formation during autophagy, and Beclin protein plays a crucial role in autophagy activation by regulating the nucleation of autophagic vesicles.[32] Hence,

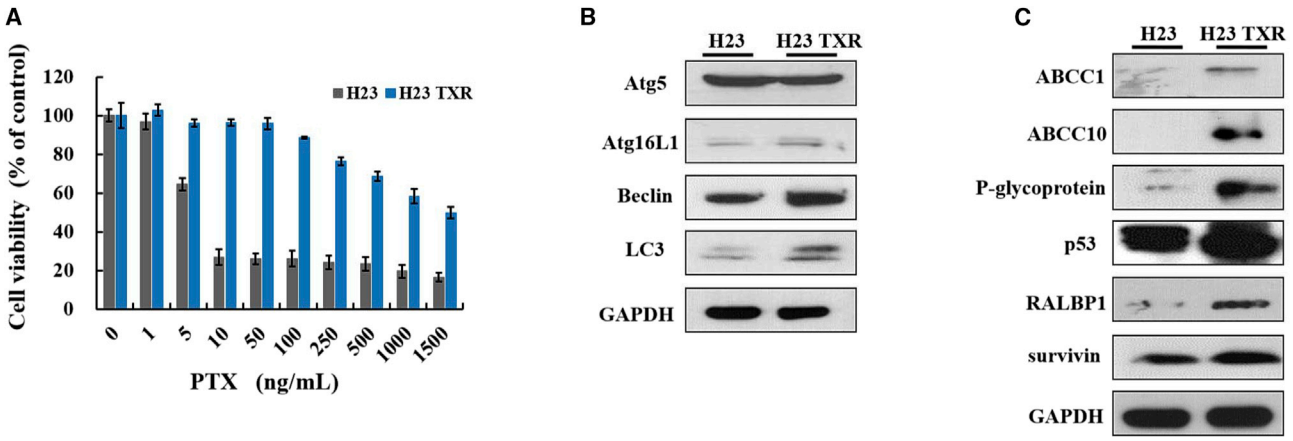

Figure 1. Characterizing Differences between Paclitaxel-Resistant NCI-H23-TXR Cells and Parental NCI-H23 Cells

(A) Relative cell viabilities of cells exposed to various PTX concentrations (1–1,500 ng/mL) for 3-day incubation at 37°C using MTT assay (n = 8). (B) Expression levels of autophagy-related proteins in cells. (C) Expression levels of MDR-related proteins, P53, and survivin in cells. Cell lysates were extracted, and protein expression was detected by western blot. GAPDH was used as an internal control for equal loading.

Beclin-siRNA was selected to inhibit autophagy protein expression because Beclin is upstream of LC3. The western blot assay was also applied to identify differentially MDR-expressed proteins in cell lines. Compared with NCI-H23 cells, NCI-H23-TXR cells showed high expression levels in P-gp, multidrug resistance protein 7 (MRP7), a sub-family C member 10 encoded in humans by the ABCC10 gene, and the RALBP1, a non-ATP-binding cassette (ABC) transporter associated with MDR (Figure 1C).

Intracellular Uptake and Knockdown Efficiency of CS-PEI/siRNA

Fluorescein isothiocyanate (FITC)-labeled CS-PEI was utilized for cellular uptake in PTX-resistant and parental cells. In Figures 2A and 2B, both flow cytometric and confocal laser scanning microscopic (CLSM) results clearly demonstrate that NCI-H23 and NCI-H23-TXR cells had similar abilities in internalization of the CS-PEI/siRNA polyplex at N/P = 5. After confirming the cellular uptake of the polyplex in cells, we examined whether the CS-PEI/Beclin-siRNA polyplex could suppress Beclin expression in NCI-H23-TXR cells. Cells were treated with the polyplex for 4 h, and non-internalized polyplex particles were then washed out, followed by post-incubation of siRNA-treated cells for 0–2 days. As shown in Figure 2C, the expression level of Beclin in NCI-H23-TXR cells treated with Beclin-siRNA was similar to that in parental NCI-H23 cells without post-incubation and increased with prolonged post-incubation time. The expression levels of Beclin in NCI-H23-TXR cells were 0.56, 0.73, and 0.77 for post-incubation times of 0, 1, and 2 days, respectively. Accordingly, the expression levels of MDR-related proteins in the resistant cells also increased with prolonged post-incubation time. They were 0.66, 0.75, and 0.82 for ABCC10; 0.50, 0.56, and 0.77 for P-gp; and 0.46, 0.57, and 0.76 for RaLBP1 at post-incubation days 0, 1, and 2, respectively.

To reconfirm whether the recovery of Beclin-siRNA-transfected NCI-H23-TXR cells was truly time dependent, we performed quantitative real-time PCR analyses to measure the expression of mRNA. Similar to western blot analysis results, the mRNA levels of Beclin, P-gp, and ABCC10 were suppressed when NCI-H23-TXR cells were treated with Beclin-siRNA without post-incubation, but renewed with the prolonged post-incubation time (Figure 2D).

A commercial gene vector jet-PRIME that also contains PEI segments was selected as a reference group. As shown in Figure 3A, both CS-PEI and jet-PRIME led to the recovery of Beclin expression in scrambled siRNA-transfected NCI-H23 cells and Beclin-siRNA-transfected NCI-H23-TXR cells when the post-incubation time was extended from 0 to 1 or 2 days. The cell viabilities of CS-PEI/siRNA at N/P = 5 were significantly higher than those of jet-PRIME and Lipofectamine 2000 (Lipo2000) (Figure 3B), implying that CS-PEI had the lowest cytotoxicity.

Figure 3C shows the cell viabilities of NCI-H23 cells treated with various concentrations of PTX for 3 days post-incubation and those of NCI-H23-TXR cells exposed to PTX for 3 days post-incubation with or without pretreatments of Beclin-siRNA for 4 h followed by post-incubation of 0, 1, and 2 days. The percentages of viable cells decreased dramatically in NCI-H23 cells with increasing PTX concentrations but remained intact in NCI-H23-TXR cells even at a high PTX concentration of 250 ng/mL. Among the drug-resistant test groups, the percentages of viable cells decreased markedly when the cells were pretreated with Beclin-siRNA for 4 h and treated with PTX at concentrations exceeding 100 ng/mL. The cell-killing ability of PTX decreased in Beclin-siRNA-treated NCI-H23-TXR cells with prolonged incubation time. The IC_{50} values of PTX against NCI-H23-TXR cells were 1,296, 255.8, 659.3, and 754.2 ng/mL, corresponding to those samples without any treatment and with Beclin-siRNA treatments for 0, 1, and 2 days post-incubation, respectively. These results are consistent with findings previously obtained using western blot (Figure 2C), that

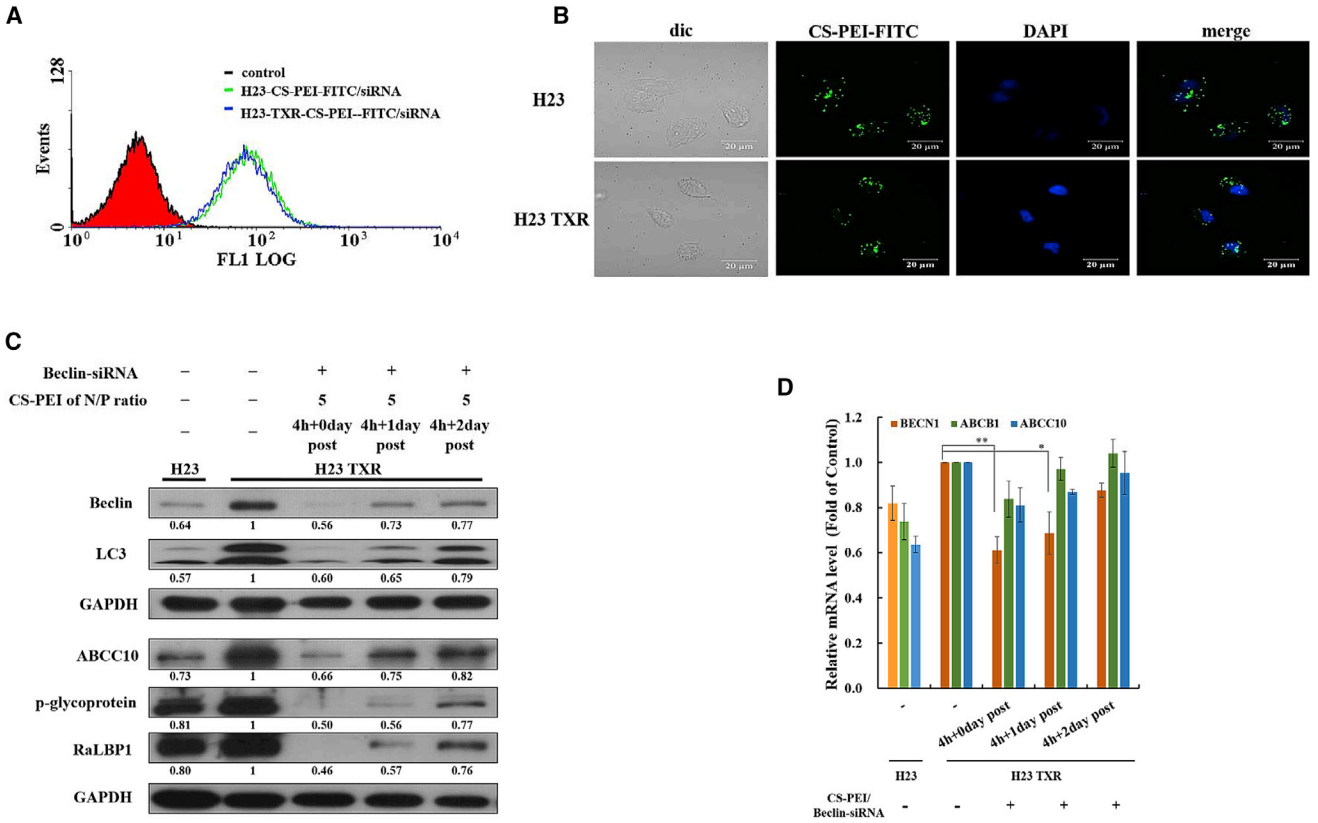

Figure 2. Knockdown Efficiency of siRNA Using CS-PEI as a Vector

(A) Internalization of a polyplex into NCI-H23 and NCI-H23-TXR cells. The polyplex was prepared from FITC-conjugated CS-PEI and scrambled siRNA at N/P = 5. Green fluorescence intensities of CS-PEI-FITC/siRNA polyplex in cells were detected at 4-h incubation using flow cytometry. (B) CLSM images of NCI-H23 and NCI-H23-TXR cells exposed to CS-PEI-FITC/siRNA polyplex at N/P = 5 for 4 h. Green: FITC-conjugated CS-PEI; blue: DAPI-stained cell nuclei. (C) Western blot analysis of autophagy- and MDR-related protein expression levels of cells with different treatments. NCI-H23-TXR cells were transfected with CS-PEI/Beclin-siRNA at N/P = 5 for 4 h followed by 0, 1, and 2 days post-incubation. Cell lysates were extracted and detected by western blot. Protein ratios were calculated from western blot images using ImageJ software and compared with NCI-H23 TXR cells. GAPDH was used as an internal control for equal loading. (D) Relative mRNA levels of gene expression of Beclin, P-glycoprotein, and ABCC10 in siRNA-treated cells using quantitative real-time PCR. Levels of mRNA were normalized to endogenous GAPDH gene and presented with a mean value ± SD. The mean values were obtained from three different independent experiments, and statistical analysis was performed using the two-tailed Student's t test (n = 3; *$p < 0.05$, **$p < 0.01$).

is, increases in Beclin and MDR-related protein expression with prolonged post-incubation time.

Knockdown in Beclin and LC3 Expression after Phagocytosing the CS-PEI/Beclin-siRNA Polyplex

Beclin expression was upregulated and associated with LC3 in PTX-resistant NCI-H23-TXR cells. In Figure 4A, higher Beclin and LC3 expression in NCI-H23-TXR cells than in NCI-H23 cells was also observed using an immunostaining assay by CLSM. NCI-H23-TXR cells after phagocytosis of the CS-PEI/Beclin-siRNA polyplex clearly suppressed Beclin and LC3 expression compared with phagocytosis of the CS-PEI/scrambled siRNA polyplex. The levels of Beclin and LC3 expression relative to parental NCI-H23 cells were also calculated and included in Figure 4B. The suppression fold of Beclin and LC3 proteins showed a significant difference in NCI-H23-TXR cells of phagocytosing CS-PEI/Beclin-siRNA and phagocytosing CS-PEI/scrambled siRNA ($p < 0.01$).

Restored Sensitivity of NCI-H23-TXR Cells to PTX after Phagocytosing the CS-PEI/Beclin-siRNA Polyplex

An Annexin V-PI dual-staining assay was performed to examine PTX-restored cell apoptosis after cells were treated with a series of polyplexes containing scrambled siRNA or Beclin-siRNA for 4 h followed by treatment with 250 or 500 ng/mL PTX for 3 days post-incubation. As shown in Figure 5A, the four quadrants displayed necrotic cells stained with PI in the upper left quadrant (Q1), late apoptotic cells stained with PI and Annexin V in the upper right quadrant (Q2), early apoptotic cells stained with Annexin V in the lower right quadrant (Q3), and healthy cells not stained with PI and Annexin V in the lower left quadrant (Q4). The sum of Q2 and Q3 accounted for the percentage of apoptotic cells, and the Q1 value for necrotic cells was plotted as shown in Figure 5B. Obviously, the percentages of apoptotic cells increased with an increase in PTX concentration for all test groups. In comparison of the percentages of apoptotic cells,

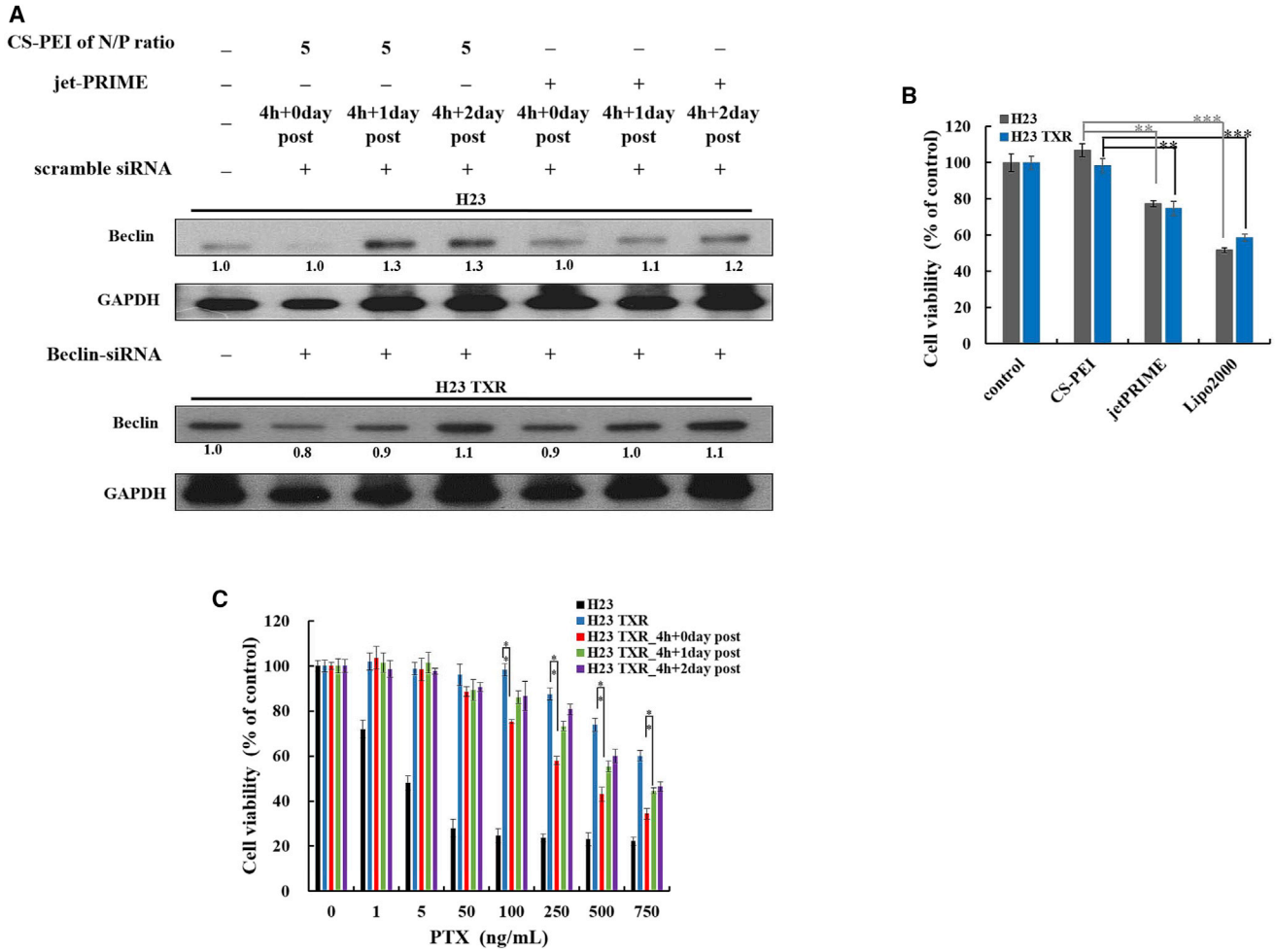

Figure 3. Levels of Beclin Expression and Cytotoxicity of Cells Treated with siRNA in a Post Time-Dependent Manner

(A) Western blot analysis of Beclin protein expression level of cells. NCI-H23 cells were transfected with CS-PEI/scramble siRNA at N/P = 5 or jet-PRIME/scramble siRNA; NCI-H23-TXR cells were transfected with CS-PEI/Beclin-siRNA at N/P = 5 or jet-PRIME/Beclin-siRNA for 4 h followed by 0, 1, and 2 days post-incubation. Cell lysates were extracted, and protein expression was detected by western blot. Protein expression levels were calculated from western blot images using ImageJ software, and the ratios were obtained relative to the control group (untreated cells). GAPDH was used as an internal control for equal loading. (B) *In vitro* cytotoxicity analysis of siRNA carried by different transfection agents using MTT assay. Cells were treated with Beclin-siRNA carried by different transfection agents for 4-h incubation. CS-PEI/siRNA was prepared at N/P = 5. Lipofectamine 2000/siRNA and jet-PRIME/siRNA were prepared according to the manufacturer's protocols. (C) Relative cell viabilities of cells treated with or without siRNA and exposed to various PTX concentrations for 3 days post-incubation using MTT assay. NCI-H23-TXR cells were transfected with CS-PEI/Beclin-siRNA at N/P = 5 for 4 h and subsequently treated with various concentrations of paclitaxel (1–750 ng/mL) at post-incubation days 0, 1, and 2. Statistical analysis was performed using the two-tailed Student's t test (n = 8; *p < 0.05, **p < 0.01, ***p < 0.001).

~95% of NCI-H23 cells and ~28% of NCI-H23-TXR cells died when cells were treated with 500 ng/mL PTX; nevertheless, the percentage of apoptotic cells increased to ~48% when NCI-H23-TXR cells were pretreated with CS-PEI/Beclin-siRNA. The PTX-restored cell apoptosis was reconfirmed by the MTT assay shown in Figure 5C.

Signaling Proteins of Apoptosis Revealed Using Micro-Western Blot Array

To compare profiling changes of signaling pathways modulated in NCI-H23 and NCI-H23-TXR cells following autophagy blocking by Beclin-siRNA, we performed the micro-western array, a high-throughput western blot array (Figure 6A). Target proteins in different signaling pathways such as apoptosis, mammalian target of rapamycin (mTOR), and PI3K/Akt were investigated on NCI-H23-TXR cells in response to CS-PEI/Beclin-siRNA transfection and PTX treatment. NCI-H23-TXR cells were transfected with CS-PEI/Beclin-siRNA at N/P = 5 for 4 h and subsequently treated with PTX at 50 ng/mL for 1 day. Protein abundance was normalized to the average of actin. In view of delicate differences in experimental findings, the results obtained from micro-western array were reconfirmed using traditional western blot analysis (Figure 6B). The expression levels of autophagy-, MDR-, and apoptosis-related protein of

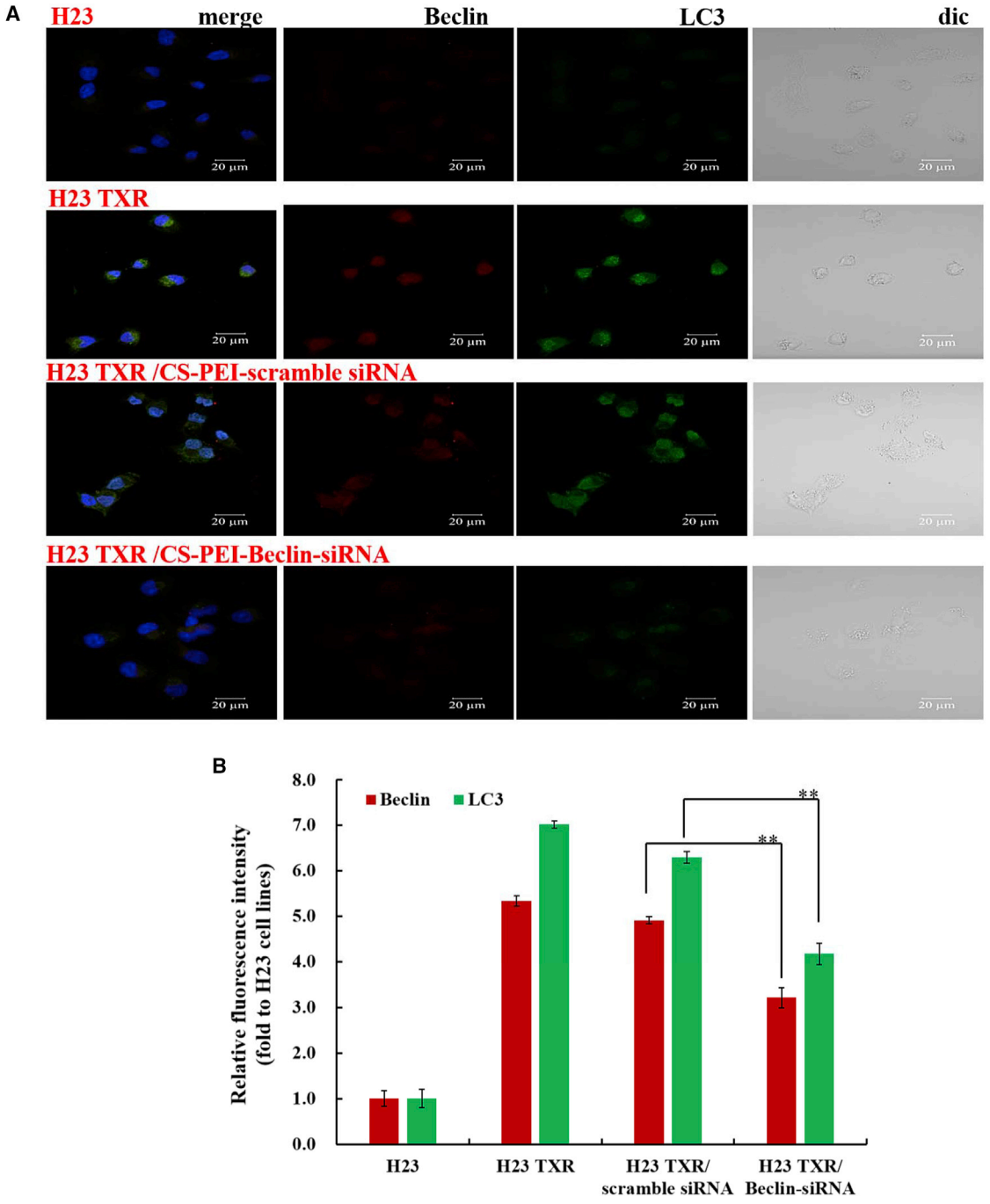

Figure 4. Localization and Quantification of Autophagy-Related Proteins

(A) CLSM images of Beclin and LC3 expression in CS-PEI/siRNA-transfected NCI-H23-TXR cells at N/P = 5 for 4 h. After incubation, cells were stained with anti-Beclin and anti-LC3 antibody using an immunofluorescence staining method. Red: Beclin expression; green: LC3 expression; blue: DAPI-stained cell nuclei. Scale bar, 20 μm. (B) Relative fluorescence intensities of Beclin and LC3 calculated from the immunofluorescence staining images using ZEISS ZEN Microscope software and compared with those of NCI-H23 cells. Statistical analysis was performed using the two-tailed Student's t test (n = 3; *$p < 0.05$, **$p < 0.01$).

cells with different treatments were calculated from western blot images using ImageJ software and compared with NCI-H23 TXR cells. The relative values of protein expression obtained from three different independent experiments were presented as bar graphs as shown in Figure 6C. The precursor forms of pro-apoptotic caspase-3, caspase-9, and the cleavage of poly(ADP-ribose) polymerase

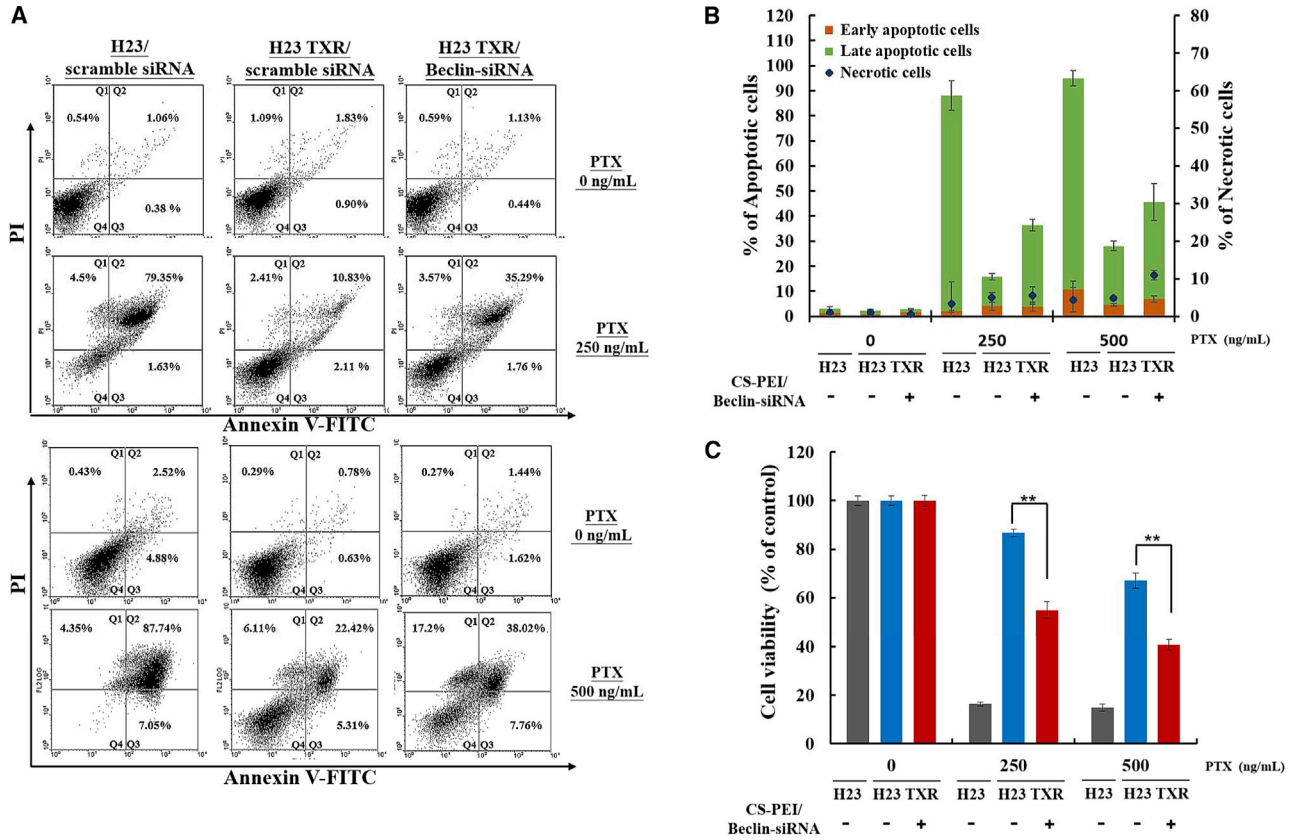

Figure 5. Induction of Apoptosis in NCI-H23 and NCI-H23-TXR Cells Exposed to Various Concentrations of Paclitaxel (PTX)

(A) Annexin V-PI (propidium iodide) dual-staining assay by flow cytometry analysis. Cells were transfected with CS-PEI/siRNA at N/P = 5 for 4 h followed by treatments with various concentrations of PTX (0, 250, and 500 ng/mL). After 3 days of incubation in PTX, the treated cells were collected and co-stained with Annexin and PI dye. The results were acquired from each sample consisting of 10,000 cells using flow cytometry. The values in the upper left quadrant (Q1), upper right quadrant (Q2), lower right quadrant (Q3), and lower left quadrant (Q4) represent the relative amount of necrotic, late apoptotic, early apoptotic, and live cells, respectively. (B) Percentages of apoptotic cells based on the results from (A) (n = 3). (C) Relative cell viabilities of cells treated with CS-PEI/Beclin-siRNA followed by exposure to various PTX concentrations for 3 days post-incubation. Statistical analysis was performed using the two-tailed Student's t test (n = 8; *$p < 0.05$, **$p < 0.01$).

(PARP) were remarkably enhanced as NCI-H23-TXR cells were pre-transfected with CS-PEI/Beclin-siRNA.

In Vivo Tumor Suppression in Zebrafish Embryos

Zebrafish (*Danio rerio*) is an ideal model organism with several advantages, including transparent embryos, small size, and rapid development.[33,34] Zebrafish-based tumor xenograft assay has recently become a useful tool for examining *in vivo* invasion, proliferation, and angiogenesis of xenografted tumors of human cancer cells.[35,36] Initially, the tolerance level of zebrafish to PTX concentrations was tested. The results showed that treatments of PTX ranging within 0.5–10 μg/mL did not affect the survival rate of zebrafish larvae at 1 or 2 days post-fertilization (Figures S4A and S4B). To further validate inhibition of autophagy in suppression of tumor growth in NCI-H23-TXR-xenografted tumors with PTX treatments, we performed the zebrafish tumor xenograft assay. The injected tumor cells were pre-stained with a red fluorescent dye using a PKH26 Red Fluorescent Cell Linker Kit for clear observation. Figure 7A shows the fluorescent images of siRNA-transfected tumors in zebrafish treated with or without PTX and the tumor volume distribution in zebrafish embryos. The fluorescent area was observed under fluorescent microscopy and analyzed using ImageJ software; the quantitative values of tumor volumes were presented in bar graphs as shown in Figure 7B. The fluorescent images of tumor sites were also enlarged for easy calculation of tumor volumes (Figure S4C). The mean fluorescent area was also presented in dot plot using GraphPad Prism 5 software (Figure S4D). The results clearly demonstrated that inhibition of autophagy using Beclin-siRNA significantly restored the sensitivity of NCI-H23-TXR to PTX, whereas scrambled control did not.

Direct Knockdown in MDR Proteins and Restored Sensitivity of NCI-H23-TXR Cells to PTX

Knockdown of Beclin simultaneously suppressed expression of MDR-related proteins in NCI-H23-TXR cells; hence, P-glycoprotein siRNA (PGP-siRNA) was selected to knock down P-gp and to see whether the direct inhibition of MDR would restore higher cell-killing

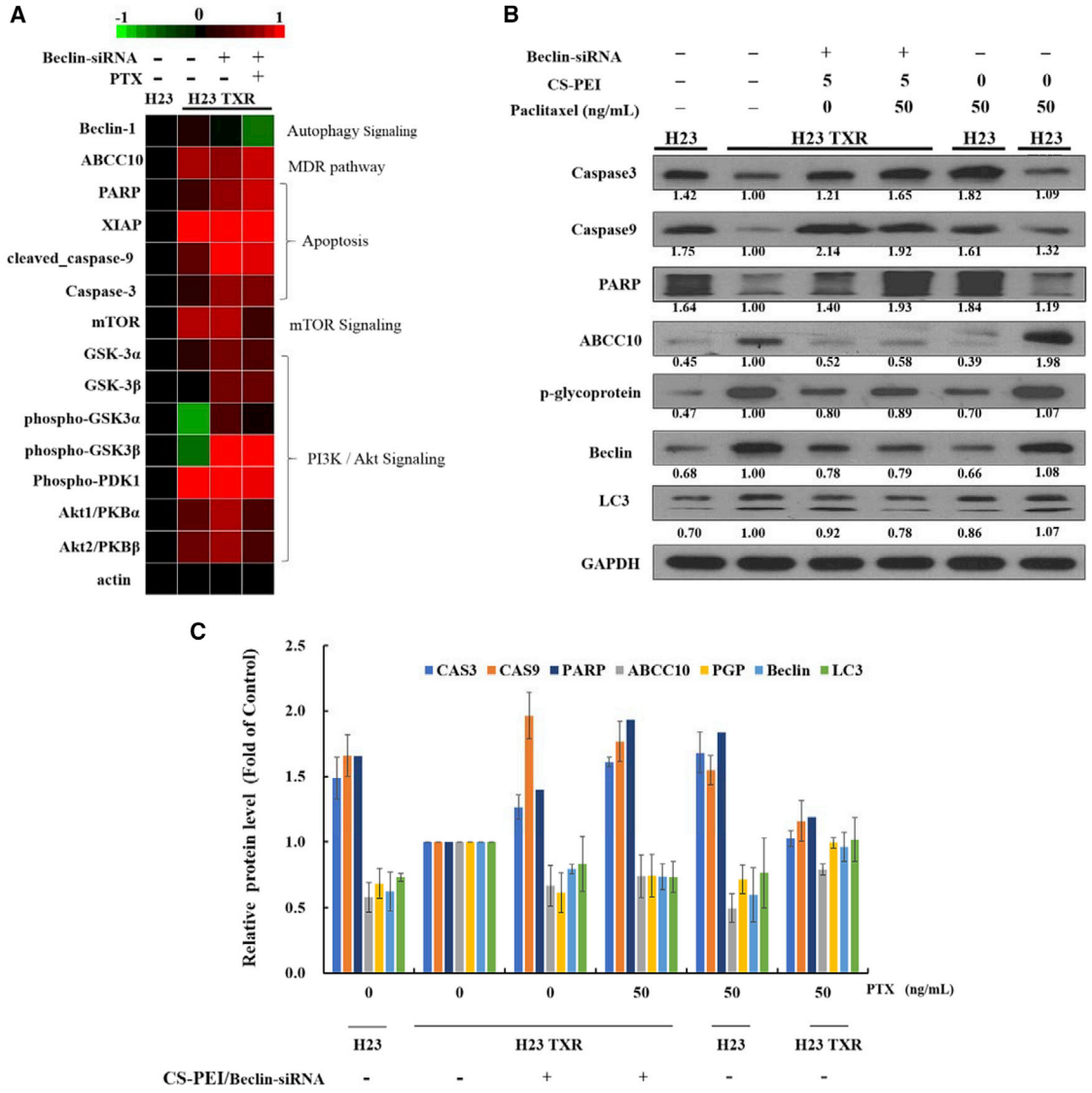

Figure 6. Regulation of Cell Proliferation Genes of NCI-H23 and NCI-H23-TXR Cells

(A) Micro-western array analysis of gene expression. Target proteins in different signaling pathways such as apoptosis, mTOR, and PI3K/Akt were investigated on NCI-H23-TXR cells in response to CS-PEI/Beclin-siRNA transfection and paclitaxel (PTX) treatment. NCI-H23-TXR cells were transfected with CS-PEI/Beclin-siRNA at N/P = 5 for 4 h and subsequently treated with PTX at 50 ng/mL for 1 day. Expression intensity levels were displayed on the top from green color (the lowest expression) to red color (the highest expression); black color indicates no change. Protein abundance was normalized to the average of actin. (B) Western blot analysis of autophagy-, MDR-, and apoptosis-related protein expression levels of cells with different treatments. Cell lysates were extracted from siRNA-transfected and PTX-treated cells, and protein expression was detected by western blot. GAPDH was used as an internal control for equal loading. Protein expression levels were calculated from western blot images using ImageJ software, and the ratios were obtained relative to NCI-H23 TXR cells. (C) Relative protein expression levels obtained from three different independent experiments in bar graphs (n = 3).

ability of PTX against NCI-H23-TXR cells. Figure 8A displays western blot results, clearly showing downregulation of Beclin and P-gp expression when NCI-H23-TXR cells were transfected with CS-PEI/PGP-siRNA at N/P = 5 and jet-PRIME/PGP-siRNA for 4 h using *GAPDH* as an internal control for equal loading. Beclin and LC3 expression levels were 0.46 and 0.45 with CS-PEI and 0.49 and 0.47 with jet-PRIME, implying a similar transfection efficacy in the use of both gene delivery vectors. Figure 8B shows inhibition of cell proliferation after treatment of cells with Beclin-siRNA and PTX. Figure 8C displays cells treated with PGP-siRNA and PTX. Similarly restored cell-killing ability of PTX in NCI-H23-TXR cells was observed regardless of whether using Beclin-siRNA to knock down the autophagy gene or using PGP-siRNA to knock down the MDR gene directly.

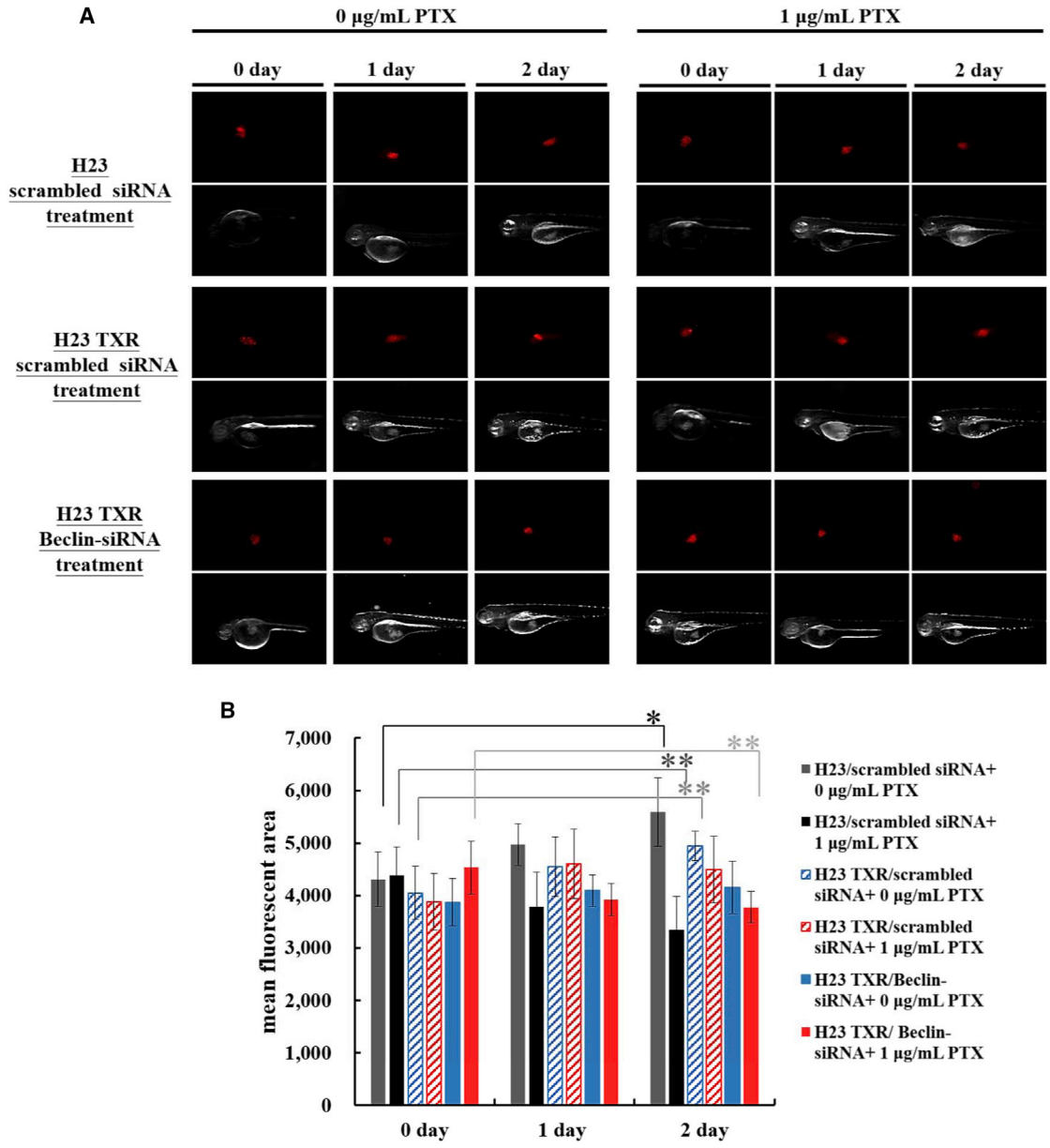

Figure 7. Paclitaxel (PTX) Inhibition on Tumor Growth in Zebrafish Tumor-Xenograft Model

(A) Fluorescent images of zebrafish tumors treated with or without PTX. The siRNA-transfected cells were pre-stained with PKH26 red fluorescent dye for clear observation. Labeled cells were injected into zebrafish using a single injection with ~850 cells per embryo. After zebrafish were treated with or without PTX dissolved in aerated water containing 1× phenylthiourea for various days (0–2 days), the fluorescent images of tumor sites were observed using fluorescent microscopy. (B) Tumor growth inhibition is presented in the bar graphs. Mean fluorescent areas of tumor sites in zebrafish were analyzed using ImageJ software, and statistical analysis was performed using the two-tailed Student's t test (n = 30; *$p < 0.05$, **$p < 0.01$).

DISCUSSION

Our previous study found an increase in green fluorescence intensity of pEGFP expression when using CS-PEI as a plasmid DNA (pDNA) delivery vector with increased post-incubation time in glioblastoma U87 cells by CLSM.[37] In contrast, this study found that NCI-H23-TXR cells treated with Beclin-siRNA and with prolonged post-incubation time re-sensitized autophagy and MDR proteins, and decreased therapeutic activity of PTX. The contradicting result obtained in delivery of pDNA and siRNA using the same carrier might be because of their intrinsic properties. Prolonging circulation of siRNA in the cytoplasm might cause serious degradation compared with pDNA, leading to a decrease in transfection activity. Another possible reason is that Beclin expression is restored in proliferating cells. Brower et al.[38] reported that the doubling time of NCI-H23 cells

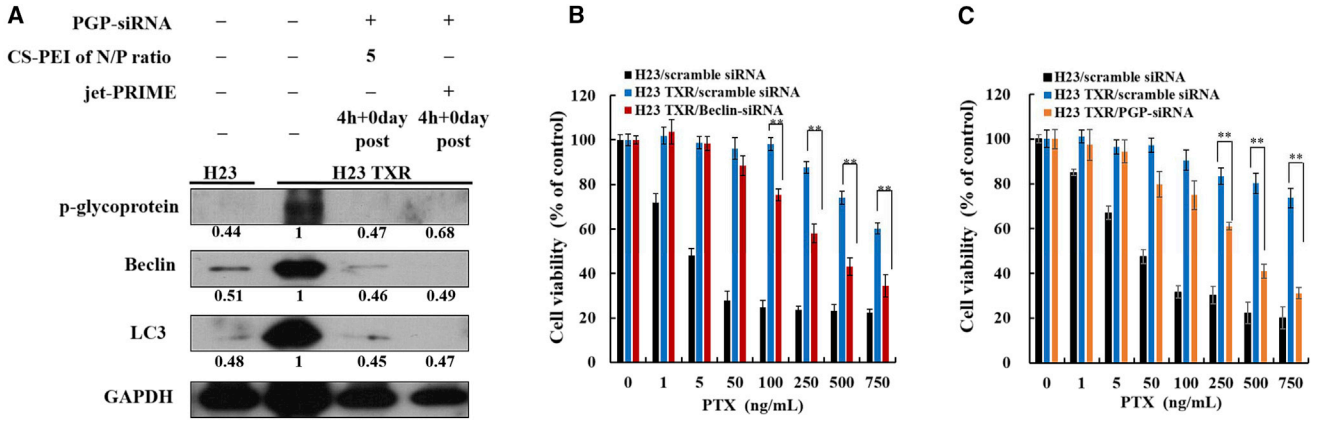

Figure 8. Downregulation of Protein Expression in Cells Treated with CS-PEI/P-Glycoprotein siRNA

(A) P-glycoprotein (PGP) expression levels of NCI-H23 cells and NCI-H23-TXR cells analyzed by western blot. NCI-H23-TXR cells were transfected with CS-PEI/PGP siRNA at N/P = 5 and jet-PRIME/PGP siRNA for 4 h. Cell lysates were extracted from siRNA-transfected cells, and protein expression was detected using western blot. Protein ratios were calculated from western blot images using ImageJ software relative to NCI-H23 TXR cells. GAPDH was used as an internal control for equal loading. (B and C) Relative cell viabilities of cells exposed to different CS-PEI/siRNA polyplexes at N/P = 5 for 4 h and subsequently treated with various concentrations of paclitaxel (1–750 ng/mL) for 3 days post-incubation. The cells were treated with (B) CS-PEI/Beclin-siRNA and (C) CS-PEI/PGP-siRNA. Statistical analysis was performed using the two-tailed Student's t test (n = 8; *p < 0.05, **p < 0.01).

in RPMI containing 10% fetal bovine serum (FBS) was 38 h. Thus, the restored Beclin expression went hand in hand with the amount of new proliferating NCI-H23-TXR cells as the incubation time was extended.

In another study, Wang et al.[39] have found that PEI induced cytotoxicity and promoted Beclin expression, leading to degradation of PEI-alginate nanoparticles (PEI-Alg NPs) in endothelial progenitor cells. The intense phagocytosis and subsequent turnover of membrane structures caused severe oxidative stress and cell apoptosis. The authors concluded that administration of PEI-Alg NPs in appropriate concentrations should be ascertained to avoid occurrence of severe oxidative stress during phagocytosis. Because CS and alginate are all naturally derived polysaccharides, the same explanation might be adapted here for CS-PEI as an siRNA carrier. Nevertheless, compared with jet-PRIME and Lipo2000, CS-PEI is beneficially indicated to be a better gene carrier because of a lower cytotoxicity.

3-Methyladenine and chloroquine have been used as inhibitors to directly inhibit autophagy proteins sensitizing MDR-phenotype ovarian cancer SKVCR cells to vincristine treatment.[25] Autophagy-promoted PTX resistance has also been reported on cervical cancer cells, where the Warburg effect activating hypoxia-induced factor 1-alpha-mediated signaling is involved.[15] Although direct reduction of autophagy expression by inhibitors seems to be a straightforward strategy, such a strategy is associated with a toxic problem at the dosage of inhibitors required to attenuate autophagy function in clinical settings.[4,7] Alternatively, the use of autophagy-related siRNA to regulate programmed cell death in MDR cells seems attractive.

According to western blot results, an increased expression level of Beclin corresponded with the expression levels of MRD proteins like P-gp, ABCC10, and RALBP1, indicating the association of autophagy and MDR proteins. Knockdown of Beclin expression simultaneously suppresses MDR-related proteins, leading to increasing cellular uptake of a chemotherapy drug and resulting in better therapeutic outome.[26] NCI-H23-PTX cells pretreated with Beclin-siRNA intercepted the autophagy pathway and simultaneously regulated MDR protein expression, leading to restored sensitivity of cells to PTX. Although mechanisms underlying autophagy and MDR are not fully understood, several studies have demonstrated that autophagy promotes the development of MDR.[20,40,41] P-gp and ABCC10 are the ABC-transporter efflux proteins associated with MDR activity in cancer. Overexpression of P-gp occurs frequently to resistance against a wide variety of chemotherapeutic agents.[42] However, Oguri et al.[43] found higher gene expression levels of both P-gp and ABCC10 in PTX-resistant NSCLC PC-6/TAX1-1 cells than those in parental PC-6 cells. The expression levels of ABCC10 showed significantly negative correlation with PTX sensitivity in 17 NSCLC cells, compared with the expression levels of P-gp; therefore, the authors suggested using ABCC10 instead of the commonly used P-gp as the biomarker for PTX resistance in NSCLC diseases. Moreover, high expression level of RALBP1 (RLIP76) in PTX-resistant cells relative to parental cells was also found in NCI-H23-TXR cells. RALBP1 is a ubiquitous protein present in humans and is also one of the non-ABC transporter proteins frequently associated with MDR. It has been reported that RALBP1 is the major transporter of doxorubicin (DOX) in lung cancer cells[44] and colorectal cancer cells.[45] Nevertheless, this is the first example found in PTX-resistant NSCLC cells.

Autophagy can protect cancer cells during chemotherapy, leading to cancer drug resistance. The results of micro-western array analysis indicated several signaling proteins involved in PTX-resistant cells

pretreated with Beclin-siRNA, suggesting that inhibition of Beclin re-sensitizes NCI-H23-PTX cells to PTX. Beclin re-sensitizing NCI-H23-PTX cells to PTX is majorly involved in caspase-3 and caspase-9 apoptosis pathways. mTOR also plays an important role in regulating apoptosis through suppressing phosphorylation of the Akt family.[46]

A zebrafish-based xenograft tumor was successfully established to screen NCI-H23 and NCI-H23-TXR tumors with and without Beclin-siRNA knockdown, as well as with and without PTX treatment. All results were consistent with the findings in the cell; that is, the inhibition of autophagy using Beclin-siRNA significantly restores the sensitivity of NCI-H23-TXR to PTX.

Autophagy facilitated the development of MDR in NCI-H23-TXR cells, leading to inhibition of apoptosis. Subsequently, we were interested in whether direct inhibition of MDR using PGP-siRNA would restore higher cell-killing ability of PTX against NCI-H23-TXR cells. Nevertheless, the results demonstrated the restored PTX ability in killing NCI-H23-TXR cells was similar in inhibition to an autophagy-related Beclin gene and a MDR-related P-gp gene. Both P-gp and Beclin are mainly involved in the development of MDR in NCI-H23-TXR cells. The relationship between autophagy and MDR is complicated and still needs clarification. Here, we demonstrated that combinations of PTX either with MDR inhibitors like PGP-siRNA or with knockdown autophagy genes like Beclin-siRNA are all promising strategies for lung cancer treatment in the future.

Conclusions

CS-PEI seems to be a potent gene delivery vector because of comparable knockdown efficiency with lower cytotoxicity than commercial products jet-PRIME and Lipo2000. Distinct Beclin expression of autophagy level was observed in NSCLC of NCI-H23-TXR and parental NCI-H23 cells. Knockdown of the Beclin gene simultaneously inhibited MDR-related proteins and restored the sensitivity of NCI-H23-TXR cells to PTX. A zebrafish-based xenograft tumor model was successfully established, and NCI-H23-TXR tumor sizes could be suppressed when zebrafish were pretreated with CS-PEI/Beclin-siRNA followed by PTX treatments. The restored PTX ability in killing NCI-H23-TXR cells was similar in inhibition to an autophagy-related Beclin gene or an MDR-related P-gp gene. This study may provide new insight for PTX chemo-resistant therapy in NSCLC.

MATERIALS AND METHODS

Materials

PEI was purchased from Polyscience (Warrington, PA, USA), and CS was from Tohoku Miyagi Pharmaceutical (Tokyo, Japan). FITC and MTT were from Sigma-Aldrich (St. Louis, MO, USA). PTX was purchased from TCI (Tokyo, Japan) and dissolved in DMSO (Sigma Aldrich) at a concentration of 10 mg/mL as a stock solution and stored at −20°C for further use. Beclin-siRNA and scrambled siRNA were purchased from GE Dharmacon (Lafayette, CO, USA). PEI was chemically grafted onto CS via Michael addition to yield CS-PEI copolymers.[29] FITC-labeled CS-PEI for cell imaging was synthesized according to a reported method with slight modification.[47]

Preparation and Characterization of Polyplexes

Polyplexes were prepared with various N/P ratios of CS-PEI and siRNA using an equal volume of 250 μL serum-free medium containing various amounts of CS-PEI to adjust an N/P ratio with a fixed amount of 100 pmol siRNA. Polyplexes were formed for 30 min at room temperature. The size and morphology of polyplexes were observed by TEM (JEM-2000 EXII; JEOL, Tokyo, Japan). TEM samples were prepared as previously reported.[37]

Agarose Gel Electrophoresis

CS-PEI/siRNA was prepared with various N/P ratios of 1–9. After incubation of polyplexes for 30 min at room temperature, samples were loaded into the well of 1.2% agarose gel containing DNA safe stains dye (Leadgene Biomedical, Tainan, Taiwan) and run with Tris-acetate buffer at 160 V for 35 min. The CS-PEI/siRNA polyplex was visualized with UV light irradiation at 365 nm.

siRNA Transfection

Beclin-siRNA or scrambled siRNA was mixed with CS-PEI to form a polyplex in a serum-free medium for 30 min at room temperature. The final volume of the polyplex was adjusted to 1 mL using the same medium and then added into cells in each 12-well plate. Following 4 h of transfection, each well containing cells was replaced with 1.5 mL of fresh complete medium, and inhibition of Beclin protein expression was evaluated using western blot.

Cell Experiments

Cell Culture

NCI-H23 cells, originally from human lung adenocarcinoma, were grown in RPMI-1640 supplemented with 5% heat-inactivated FBS and 1% penicillin-streptomycin-glutamate solution in a 37°C incubator with a humidified atmosphere containing 5% CO_2. PTX-resistant subline (NCI-H23-TXR) was established *in vitro* by exposing NCI-H23 cells to gradually increased concentrations of PTX in culture medium.[27] NCI-H23-TXR cells were maintained in the culture medium with the additional presence of 10 nM PTX. Both cell lines are obtained from the National Health Research Institutes of Taiwan (NHRI).

Cell Viability

Cell viability was measured using the MTT assay. NCI-H23 and NCI-H23-TXR cells were seeded at a density of 5×10^3 cells/well in 96-well plates with RPMI-1640 medium and incubated for 24 h before transfection. Cell media containing various PTX concentrations (1–1,500 ng/mL) were added to cells and cultured at 37°C for another 1, 2, and 3 days. Following the incubation, the morphologies of cells were observed using an inverted phase-contrast microscope. Subsequently, each well containing cells was added with the MTT solution as previously reported.[37] The cytotoxicities of polyplexes were examined at various N/P ratios of CS-PEI/siRNA for 24 h after cells had been incubated at 37°C for 24 h. The jet-PRIME/siRNA

polyplex was prepared according to the manufacturer's protocol (Polyplus-transfection, NY, USA).

Western Blot Analysis

Cell lysates were extracted from siRNA-treated cells at 0–2 days of incubation, washed twice with 1× PBS, and resuspended in radioimmunoprecipitation assay (RIPA) buffer (71009; Merck, Darmstadt, Germany). Protein expression was determined using a protein assay kit (Bio-Rad Laboratories, Hercules, CA, USA) according to the manufacturer's protocol. Equal amounts of protein samples were separated using SDS-PAGE and transferred onto PVDF (polyvinylidene difluoride) membranes (Merck Millipore Life Science). The membranes were blocked for 3 h at room temperature with 5% non-fat milk in PBS with Tween 20 and incubated with primary antibodies at 4°C overnight. Primary antibodies were against Beclin, LC3, Atg5, and Atg16L1, respectively (1:1,000; Cell Signaling Technology, Danvers, MA, USA), p53 (1:200; Abcam, Cambridge, UK), survivin (1:1,000; Abcam), P-gp (1:500; GeneTex, Irvine, CA, USA), ABCC10 (1:200; Abcam), and GAPDH (1:10,000; GeneTex). The signals of immunoreactive blots were detected using the Enhanced Chemi-Luminescence (ECL) western blotting reagent (Perkin-Elmer, Waltham, MA, USA).

Flow Cytometry Analysis

FITC-conjugated CS-PEI was utilized to complex siRNA. Cells were transfected with FITC-CS-PEI/siRNA at the N/P ratio of 5 and incubated at 37°C for 4 h, followed by replacement with 1.5 mL fresh medium, the same method for siRNA expression. After washing three times with 1× PBS, the count of 1×10^4 cells from cell samples was collected, fixed with 4% paraformaldehyde, and analyzed using the flow cytometer (Beckman Coulter, Brea, CA, USA) with single laser at 488-nm excitation.

Immunofluorescence Staining and CLSM

Cells were transfected with or without CS-PEI/siRNA at 37°C for 4 h followed by replacement of fresh medium as aforementioned for siRNA expression. Cells grown on coverslips were washed with 1× PBS and fixed with 4% paraformaldehyde for 10 min at room temperature and then rinsed with 1× PBS three times. Subsequently, cells on coverslips were treated with 0.2% Triton X-100 (Sigma-Aldrich) for 10 min and then washed with 1× PBS three times again. Non-specific reaction was blocked with blocking buffer (4% BSA in PBS) for 1 h at room temperature. After blocking, the buffer was removed, and cells were then incubated with Beclin monoclonal primary antibody (1:100; OriGene Technologies, Rockville, MD, USA) and LC3 primary antibody (1:100; Cell Signaling Technology) at 4°C overnight. After washing three times with 1× PBS, cells were stained with both Alexa Fluor 488-tagged secondary antibody (1:100; Cell Signaling Technology) and Alexa Fluor 594-tagged secondary antibody (1:100; Cell Signaling Technology) for 1 h at room temperature. For nucleus labeling, cells were incubated with DAPI solution (Sigma-Aldrich) for 10 min at room temperature. After washing with 1× PBS for three times, the coverslip with cells was mounted with Mounting Medium (Bio-Rad Laboratories) for CLSM observation (LSM 700; Zeiss Confocal Microscopy, Stockholm, Sweden).

Annexin V-PI Staining Assay

Annexin V-PI staining assay was performed to measure cell apoptosis. Cells were transfected with or without CS-PEI/siRNA at 37°C for 4 h followed by replacement of 1.5 mL of fresh complete medium containing 250 or 500 ng/mL PTX for another 72 h post-incubation. Cultured cells were used as the blank and control groups. Following 72 h post-incubation, the Annexin V-PI staining kit (Strong Biotech, Taipei, Taiwan) was utilized. Subsequently, cell pellets were trypsinized and resuspended in binding buffer with both Annexin V-FITC and PI dye at 37°C for 30 min and analyzed using flow cytometry. The experiment was repeated three times.

Reverse Transcription and Quantitative Real-Time PCR

Cells were transfected with siRNA at 37°C for 4 h as aforementioned for siRNA transfection. After 0–48 h post-incubation, total cellular RNA was isolated using a Total RNA Miniprep Purification kit (GMbiolab, Taipei, Taiwan) according to the manufacturer's protocol. Subsequently, 200 ng RNA was used for reverse transcription into cDNA at 25°C for 10 min, 37°C for 120 min, and 85°C for 5 min with random primer using High-Capacity cDNA Reverse Transcription Kits (ABI, Warrington, UK). Quantitative real-time PCR was performed using SYBR Green PCR Master Mix (ABI). The primer sequences are as follows: for BECLIN1, forward 5′-CTGGACACTCAGCTCA ACGTCA-3′ and reverse 5′-CTCTAGTGCCAGCTCCTTTAGC-3′; for ABCB1, forward 5′-CGTGGTTGGAAGCTAACCCT-3′ and reverse 5′-TGCTGCCAAGACCTCTTCAG-3′ ; for ABCC10, forward 5′-CCTAGTGCTGACCGTGTTGT-3′ and reverse 5′-TAGGTTGG CTGCAGTCTGTG-3′ ; for GAPDH, forward 5′-GGTATCGTGGA AGGACTCATGAC-3′ and reverse 5′-ATGCCAGTGAGCTTCC CGT-3′. The amplification procedure consisted of 95°C for 20 min, followed by 40 cycles of 95°C for 3 s and 60°C for 30 s. The relative levels of target gene expression were normalized against the endogenous gene of GAPDH.

Micro-Western Blot Array

The high-throughput micro-western blot array was performed at the Micro-Western Array core facility of NHRI of Taiwan as previously described.[48] In brief, cell lysates were extracted from siRNA-treated cells after 4 h of incubation, washed twice with 1× PBS, and resuspended in 1× lysis buffer. The system of the NHRI core facility features a high-throughput screen of 48 target proteins of samples. Each micro-western blot, containing 96 individual western blots, was detected with 0.2 μL antibody and 50 nL sample, and these samples were placed with the ladder consecutively in wells of a 96-well plate in one experiment.

Zebrafish Handling and Xenograft Assay

A zebrafish xenograft assay was performed to evaluate the cytotoxic effect of PTX on drug-resistant cells through Beclin-siRNA treatments. After transfection of siRNA in NCI-H23 or NCI-H23-TXR cells, the cells were labeled with a fluorescent dye using a PKH26 Fluorescent Cell Linker Kit (Sigma Chemical) in accordance with the manufacturer's protocol. The siRNA-treated cells were stained using the PKH26 dye for 10 min at room temperature followed by

centrifugation at 1,200 rpm for 5 min and removal of the supernatant. The pellet was resuspended in media and washed twice with 1× PBS again, then subsequently suspended in 1× PBS for injection into the embryos. Zebrafish embryos at 2 days post-fertilization were dechorionated using 1 mg/mL Pronase for 5-min incubation and then anesthetized with 0.01% of tricaine. The labeled cells were transplanted in a single injection with ~850 tumor cells per embryo. The larvae recovered for 2 h at 28°C after microinjection and were then incubated in water containing 0.003% 1-phenyl-2-thiourea at 1 μg/mL PTX for 24 or 48 h post-injection in an incubator at 34°C, the optimized temperature for zebrafish and tumor growth.[49] Control embryos were treated with an equivalent amount of DMSO alone. Photographs of red fluorescence in embryos were taken using an inverted microscope, and the segmentation was quantitated in ImageJ software using threshold function for automated measurement of tumor area in yolk.

Statistical Analysis

All data were repeated at least three times from three independent experiments for analysis and presented as the mean ± SE. Student's t test was performed to determine the statistical significance of the respective group. *$p < 0.05$ or **$p < 0.01$ indicated a significant difference.

SUPPLEMENTAL INFORMATION

Supplemental Information can be found online at https://doi.org/10.1016/j.omtn.2019.06.017.

AUTHOR CONTRIBUTIONS

W.L., Y.-L.L., and Y.-T.W. designed and performed the experiments. C.H. and Z.-X.L. analyzed micro-array data. W.-J.W., Y.-J.C., and C.K. analyzed the quantitative real-time PCR results. C.-C.C. and L.-F.W. coordinated this study and wrote the paper. All authors approved the manuscript and are informed of this submission.

CONFLICTS OF INTEREST

The authors declare no competing interests.

ACKNOWLEDGMENTS

We are grateful for the financial support from the Ministry of Science and Technology of Taiwan (grants MOST104-2314-B-037-006-MY3 and MOST106-2320-B-037-004-MY3). This study was also supported by Kaohsiung Medical University under grant KMU-DK108013 and by the NSYSU-KMU Joint Research Project under grant NSYSUKMU 107-P026. NCI-H23 and NCI-H23-TXR cell lines were gifted from Dr. N.Y. Shih of the NHRI of Taiwan. We appreciate the experimental support of a CLSM and a TEM provided by the Center for Research Resources and Development of Kaohsiung Medical University.

REFERENCES

1. Yeh, J.J., Hsu, W.H., Wang, J.J., Ho, S.T., and Kao, A. (2003). Predicting chemotherapy response to paclitaxel-based therapy in advanced non-small-cell lung cancer with P-glycoprotein expression. Respiration *70*, 32–35.

2. Kim, Y.D., Park, T.E., Singh, B., Maharjan, S., Choi, Y.J., Choung, P.H., Arote, R.B., and Cho, C.S. (2015). Nanoparticle-mediated delivery of siRNA for effective lung cancer therapy. Nanomedicine (Lond.) *10*, 1165–1188.

3. Georgiadis, M.S., Russell, E.K., Gazdar, A.F., and Johnson, B.E. (1997). Paclitaxel cytotoxicity against human lung cancer cell lines increases with prolonged exposure durations. Clin. Cancer Res. *3*, 449–454.

4. Wang, L., Li, H., Ren, Y., Zou, S., Fang, W., Jiang, X., Jia, L., Li, M., Liu, X., Yuan, X., et al. (2016). Targeting HDAC with a novel inhibitor effectively reverses paclitaxel resistance in non-small cell lung cancer via multiple mechanisms. Cell Death Dis. *7*, e2063.

5. Shimomura, M., Yaoi, T., Itoh, K., Kato, D., Terauchi, K., Shimada, J., and Fushiki, S. (2012). Drug resistance to paclitaxel is not only associated with ABCB1 mRNA expression but also with drug accumulation in intracellular compartments in human lung cancer cell lines. Int. J. Oncol. *40*, 995–1004.

6. Shen, J., Yin, Q., Chen, L., Zhang, Z., and Li, Y. (2012). Co-delivery of paclitaxel and survivin shRNA by pluronic P85-PEI/TPGS complex nanoparticles to overcome drug resistance in lung cancer. Biomaterials *33*, 8613–8624.

7. Gu, J., Fang, X., Hao, J., and Sha, X. (2015). Reversal of P-glycoprotein-mediated multidrug resistance by CD44 antibody-targeted nanocomplexes for short hairpin RNA-encoding plasmid DNA delivery. Biomaterials *45*, 99–114.

8. Nascimento, A.V., Singh, A., Bousbaa, H., Ferreira, D., Sarmento, B., and Amiji, M.M. (2017). Overcoming cisplatin resistance in non-small cell lung cancer with Mad2 silencing siRNA delivered systemically using EGFR-targeted chitosan nanoparticles. Acta Biomater. *47*, 71–80.

9. Lin, C.M., Kao, W.C., Yeh, C.A., Chen, H.J., Lin, S.Z., Hsieh, H.H., Sun, W.S., Chang, C.H., and Hung, H.S. (2015). Hyaluronic acid-fabricated nanogold delivery of the inhibitor of apoptosis protein-2 siRNAs inhibits benzo[a]pyrene-induced oncogenic properties of lung cancer A549 cells. Nanotechnology *26*, 105101.

10. Yu, H., Xu, Z., Chen, X., Xu, L., Yin, Q., Zhang, Z., and Li, Y. (2014). Reversal of lung cancer multidrug resistance by pH-responsive micelleplexes mediating co-delivery of siRNA and paclitaxel. Macromol. Biosci. *14*, 100–109.

11. Liu, C., Zhao, G., Liu, J., Ma, N., Chivukula, P., Perelman, L., Okada, K., Chen, Z., Gough, D., and Yu, L. (2009). Novel biodegradable lipid nano complex for siRNA delivery significantly improving the chemosensitivity of human colon cancer stem cells to paclitaxel. J. Control. Release *140*, 277–283.

12. Feng, Q., Yu, M.Z., Wang, J.C., Hou, W.J., Gao, L.Y., Ma, X.F., Pei, X.W., Niu, Y.J., Liu, X.Y., Qiu, C., et al. (2014). Synergistic inhibition of breast cancer by co-delivery of VEGF siRNA and paclitaxel via vapreotide-modified core-shell nanoparticles. Biomaterials *35*, 5028–5038.

13. Yin, T., Wang, L., Yin, L., Zhou, J., and Huo, M. (2015). Co-delivery of hydrophobic paclitaxel and hydrophilic AURKA specific siRNA by redox-sensitive micelles for effective treatment of breast cancer. Biomaterials *61*, 10–25.

14. Tang, S., Yin, Q., Su, J., Sun, H., Meng, Q., Chen, Y., Chen, L., Huang, Y., Gu, W., Xu, M., et al. (2015). Inhibition of metastasis and growth of breast cancer by pH-sensitive poly (β-amino ester) nanoparticles co-delivering two siRNA and paclitaxel. Biomaterials *48*, 1–15.

15. Peng, X., Gong, F., Chen, Y., Jiang, Y., Liu, J., Yu, M., Zhang, S., Wang, M., Xiao, G., and Liao, H. (2014). Autophagy promotes paclitaxel resistance of cervical cancer cells: involvement of Warburg effect activated hypoxia-induced factor 1-α-mediated signaling. Cell Death Dis. *5*, e1367.

16. Song, X., Narzt, M.S., Nagelreiter, I.M., Hohensinner, P., Terlecki-Zaniewicz, L., Tschachler, E., Grillari, J., and Gruber, F. (2017). Autophagy deficient keratinocytes display increased DNA damage, senescence and aberrant lipid composition after oxidative stress in vitro and in vivo. Redox Biol. *11*, 219–230.

17. Czarny, P., Pawlowska, E., Bialkowska-Warzecha, J., Kaarniranta, K., and Blasiak, J. (2015). Autophagy in DNA damage response. Int. J. Mol. Sci. *16*, 2641–2662.

18. Maiuri, M.C., Zalckvar, E., Kimchi, A., and Kroemer, G. (2007). Self-eating and self-killing: crosstalk between autophagy and apoptosis. Nat. Rev. Mol. Cell Biol. *8*, 741–752.

19. Saiyin, W., Wang, D., Li, L., Zhu, L., Liu, B., Sheng, L., Li, Y., Zhu, B., Mao, L., Li, G., and Zhu, X. (2014). Sequential release of autophagy inhibitor and chemotherapeutic drug with polymeric delivery system for oral squamous cell carcinoma therapy. Mol. Pharm. *11*, 1662–1675.

20. Sun, W.L., Lan, D., Gan, T.Q., and Cai, Z.W. (2015). Autophagy facilitates multidrug resistance development through inhibition of apoptosis in breast cancer cells. Neoplasma *62*, 199–208.

21. Eum, K.H., and Lee, M. (2011). Targeting the autophagy pathway using ectopic expression of Beclin 1 in combination with rapamycin in drug-resistant v-Ha-ras-transformed NIH 3T3 cells. Mol. Cells *31*, 231–238.

22. Shuhua, W., Chenbo, S., Yangyang, L., Xiangqian, G., Shuang, H., Tangyue, L., and Dong, T. (2015). Autophagy-related genes Raptor, Rictor, and Beclin1 expression and relationship with multidrug resistance in colorectal carcinoma. Hum. Pathol. *46*, 1752–1759.

23. Wei, M.F., Chen, M.W., Chen, K.C., Lou, P.J., Lin, S.Y., Hung, S.C., Hsiao, M., Yao, C.J., and Shieh, M.J. (2014). Autophagy promotes resistance to photodynamic therapy-induced apoptosis selectively in colorectal cancer stem-like cells. Autophagy *10*, 1179–1192.

24. Dower, C.M., Bhat, N., Wang, E.W., and Wang, H.G. (2017). Selective reversible inhibition of autophagy in hypoxic breast cancer cells promotes pulmonary metastasis. Cancer Res. *77*, 646–657.

25. Liang, B., Liu, X., Liu, Y., Kong, D., Liu, X., Zhong, R., and Ma, S. (2016). Inhibition of autophagy sensitizes MDR-phenotype ovarian cancer SKVCR cells to chemotherapy. Biomed. Pharmacother. *82*, 98–105.

26. Hung, A.C., Tsai, C.H., Hou, M.F., Chang, W.L., Wang, C.H., Lee, Y.C., Ko, A., Hu, S.C., Chang, F.R., Hsieh, P.W., and Yuan, S.S. (2016). The synthetic β-nitrostyrene derivative CYT-Rx20 induces breast cancer cell death and autophagy via ROS-mediated MEK/ERK pathway. Cancer Lett. *371*, 251–261.

27. Chatterjee, A., Chattopadhyay, D., and Chakrabarti, G. (2014). miR-17-5p downregulation contributes to paclitaxel resistance of lung cancer cells through altering beclin1 expression. PLoS ONE *9*, e95716.

28. Wang, J., Pan, X.-L., Ding, L.-J., Liu, D.-Y., Da-Peng Lei, and Jin, T. (2013). Aberrant expression of Beclin-1 and LC3 correlates with poor prognosis of human hypopharyngeal squamous cell carcinoma. PLoS ONE *8*, e69038.

29. Lo, Y.L., Sung, K.H., Chiu, C.C., and Wang, L.F. (2013). Chemically conjugating polyethylenimine with chondroitin sulfate to promote CD44-mediated endocytosis for gene delivery. Mol. Pharm. *10*, 664–676.

30. Ungaro, F., De Rosa, G., Miro, A., and Quaglia, F. (2003). Spectrophotometric determination of polyethylenimine in the presence of an oligonucleotide for the characterization of controlled release formulations. J. Pharm. Biomed. Anal. *31*, 143–149.

31. Shubayev, V.I., Pisanic, T.R., 2nd, and Jin, S. (2009). Magnetic nanoparticles for theragnostics. Adv. Drug Deliv. Rev. *61*, 467–477.

32. Wang, R.C., Wei, Y., An, Z., Zou, Z., Xiao, G., Bhagat, G., White, M., Reichelt, J., and Levine, B. (2012). Akt-mediated regulation of autophagy and tumorigenesis through Beclin 1 phosphorylation. Science *338*, 956–959.

33. Chakraborty, C., Hsu, C.H., Wen, Z.H., Lin, C.S., and Agoramoorthy, G. (2009). Zebrafish: a complete animal model for in vivo drug discovery and development. Curr. Drug Metab. *10*, 116–124.

34. Delvecchio, C., Tiefenbach, J., and Krause, H.M. (2011). The zebrafish: a powerful platform for in vivo, HTS drug discovery. Assay Drug Dev. Technol. *9*, 354–361.

35. Tat, J., Liu, M., and Wen, X.Y. (2013). Zebrafish cancer and metastasis models for in vivo drug discovery. Drug Discov. Today. Technol. *10*, e83–e89.

36. Chiu, C.-C., Chou, H.-L., Chen, B.-H., Chang, K.-F., Tseng, C.-H., Fong, Y., Fu, T.F., Chang, H.W., Wu, C.Y., Tsai, E.M., et al. (2015). BPIQ, a novel synthetic quinoline derivative, inhibits growth and induces mitochondrial apoptosis of lung cancer cells in vitro and in zebrafish xenograft model. BMC Cancer *15*, 962.

37. Lo, Y.L., Chou, H.L., Liao, Z.X., Huang, S.J., Ke, J.H., Liu, Y.S., Chiu, C.C., and Wang, L.F. (2015). Chondroitin sulfate-polyethylenimine copolymer-coated superparamagnetic iron oxide nanoparticles as an efficient magneto-gene carrier for microRNA-encoding plasmid DNA delivery. Nanoscale *7*, 8554–8565.

38. Brower, M., Carney, D.N., Oie, H.K., Gazdar, A.F., and Minna, J.D. (1986). Growth of cell lines and clinical specimens of human non-small cell lung cancer in a serum-free defined medium. Cancer Res. *46*, 798–806.

39. Wang, G.D., Tan, Y.Z., Wang, H.J., and Zhou, P. (2017). Autophagy promotes degradation of polyethyleneimine-alginate nanoparticles in endothelial progenitor cells. Int. J. Nanomedicine *12*, 6661–6675.

40. Pan, B., Chen, D., Huang, J., Wang, R., Feng, B., Song, H., and Chen, L. (2014). HMGB1-mediated autophagy promotes docetaxel resistance in human lung adenocarcinoma. Mol. Cancer *13*, 165.

41. Chittaranjan, S., Bortnik, S., Dragowska, W.H., Xu, J., Abeysundara, N., Leung, A., Go, N.E., DeVorkin, L., Weppler, S.A., Gelmon, K., et al. (2014). Autophagy inhibition augments the anticancer effects of epirubicin treatment in anthracycline-sensitive and -resistant triple-negative breast cancer. Clin. Cancer Res. *20*, 3159–3173.

42. Holohan, C., Van Schaeybroeck, S., Longley, D.B., and Johnston, P.G. (2013). Cancer drug resistance: an evolving paradigm. Nat. Rev. Cancer *13*, 714–726.

43. Oguri, T., Ozasa, H., Uemura, T., Bessho, Y., Miyazaki, M., Maeno, K., Maeda, H., Sato, S., and Ueda, R. (2008). MRP7/ABCC10 expression is a predictive biomarker for the resistance to paclitaxel in non-small cell lung cancer. Mol. Cancer Ther. *7*, 1150–1155.

44. Singhal, S.S., Singhal, J., Nair, M.P., Lacko, A.G., Awasthi, Y.C., and Awasthi, S. (2007). Doxorubicin transport by RALBP1 and ABCG2 in lung and breast cancer. Int. J. Oncol. *30*, 717–725.

45. Mollberg, N.M., Steinert, G., Aigner, M., Hamm, A., Lin, F.J., Elbers, H., Reissfelder, C., Weitz, J., Buchler, M.W., and Koch, M. (2012). Overexpression of RalBP1 in colorectal cancer is an independent predictor of poor survival and early tumor relapse. Cancer Biol. Ther. *13*, 694–700.

46. Castedo, M., Ferri, K.F., and Kroemer, G. (2002). Mammalian target of rapamycin (mTOR): pro- and anti-apoptotic. Cell Death Differ. *9*, 99–100.

47. Ma, Z., and Lim, L.Y. (2003). Uptake of chitosan and associated insulin in Caco-2 cell monolayers: a comparison between chitosan molecules and chitosan nanoparticles. Pharm. Res. *20*, 1812–1819.

48. Lin, C.Y., Huo, C., Kuo, L.K., Hiipakka, R.A., Jones, R.B., Lin, H.P., Hung, Y., Su, L.C., Tseng, J.C., Kuo, Y.Y., et al. (2013). Cholestane-3β, 5α, 6β-triol suppresses proliferation, migration, and invasion of human prostate cancer cells. PLoS ONE *8*, e65734.

49. Hamilton, L., Astell, K.R., Velikova, G., and Sieger, D. (2016). A zebrafish live imaging model reveals differential responses of microglia toward glioblastoma cells in vivo. Zebrafish *13*, 523–534.